J Fluoresc (2015) 25:87–94
DOI 10.1007/s10895-014-1483-z

ORIGINAL PAPER

Tryptophan Residue of the D-Galactose/D-Glucose-Binding Protein from *E. Coli* Localized in its Active Center Does not Contribute to the Change in Intrinsic Fluorescence Upon Glucose Binding

Olga V. Stepanenko · Alexander V. Fonin · Olesya V. Stepanenko · Maria Staiano · Sabato D'Auria · Irina M. Kuznetsova · Konstantin K. Turoverov

Received: 22 September 2014 / Accepted: 25 November 2014 / Published online: 11 December 2014

Abstract Changes of the characteristics of intrinsic tryptophan fluorescence of the wild type of D-galactose/D-glucose-binding protein from *Escherichia coli* (GGBPwt) induced by D-glucose binding were examined by the intrinsic UV-fluorescence of proteins, circular dyhroism in the near-UV region, and acrylamide-induced fluorescence quenching. The analysis of the different characteristics of GGBPwt and its mutant form GGBP-W183A together with the analysis of the microenvironment of tryptophan residues of GGBPwt revealed that Trp 183, which is directly involved in sugar binding, has the least influence on the provoked by D-glucose blue shift and increase in the intensity of protein intrinsic fluorescence in comparison with other tryptophan residues of GGBP.

Keywords Intrinsic fluorescence of proteins · Tryptophan residue · Microenvironment of tryptophan residues

Abbreviations

GGBPwt	Wild type of D-galactose/D-glucose-binding protein from Escherichia coli
GGBPwt/Glc	Complex of GGBPwt with D-glucose
PBP	Ligand-binding proteins of the bacterial periplasm

Introduction

D-Galactose/D-glucose-binding protein from *Escherichia coli* (GGBP) belongs to a class of ligand-binding proteins of the bacterial periplasm (PBP) [1–4]. These bacterial proteins participate in an active transport of the soluble molecules (for example, carbohydrates, amino acids, anions, metal ions, di-peptides and oligo-peptides, and others) inside a bacterial cell being a part of ABC transport system [3]. In some cases, these proteins are involved in chemotaxis toward substrates [5] and in bacterial quorum sensing [6].

GGBP is able to bind D-glucose and D-galactose with high affinity. This protein consists of 309 amino acids and has a typical among PBPs two-domain pattern of polypeptide chain folding (Fig. 1) [7, 1]. Both of two domains of GGBP have an α/β topology and are composed of six β-sheets framed by two or three α-helices from both sides. Protein domains are linked by hinge region organized by three separate peptide segments. The ligand-binding site for sugar binding is in the cleft between the two domains [7–11].

The Trp 183 and Phe 16 amino acid residues of GGBP ligand-binding site, belonging to different domains of the protein, form an aromatic pocket of the indole and phenol rings which incorporate a sugar molecule (Fig. 1) [10, 7]. The

Electronic supplementary material The online version of this article (doi:10.1007/s10895-014-1483-z) contains supplementary material, which is available to authorized users.

O. V. Stepanenko · A. V. Fonin · O. V. Stepanenko · I. M. Kuznetsova · K. K. Turoverov (✉)
Institute of Cytology of the Russian Academy of Sciences, Tikhoretsky ave., 4, 194064 St. Petersburg, Russia
e-mail: kkt@incras.ru

I. M. Kuznetsova · K. K. Turoverov
St. Petersburg State Polytechnical University, Polytechnicheskaya str., 29, 194064 St. Petersburg, Russia

M. Staiano · S. D'Auria
IBP-CNR, Laboratory for Molecular Sensing, Naples 111 80131, Italy

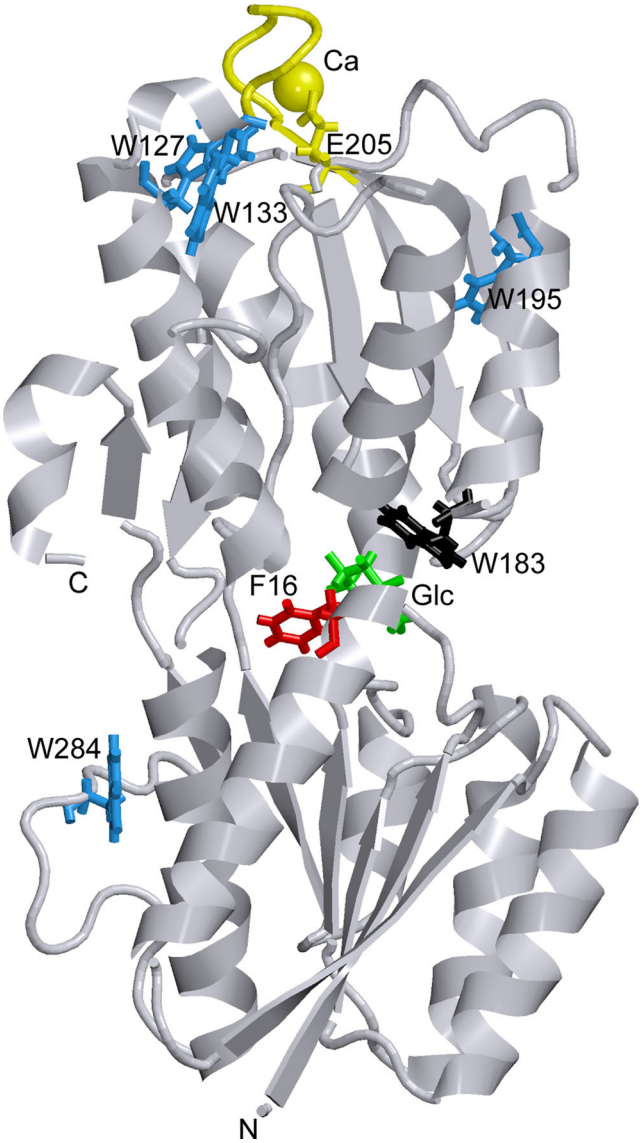

Fig. 1 Spatial structure of GGBPwt in complex with D-glucose. The tryptophan residues Trp 127, Trp 133, Trp 195 and Trp 284 are shown in *blue*. The aromatic rings of Phe 16 (*red*) and Trp 183 (*black*) sandwiching the molecule of bounded D-glucose (*green*) are drown. The Ca ion (*yellow*) is presented as van der Waals *sphere*. The residues of the Ca-binding site are shown in *yellow*, including the loop in the protein's C-terminal domain (residues 134–142) and Glu 205. The figure is created on the basis of PDB data [60] with the file 2FVY.ent [7] using the graphical software VMD [61] and Raster 3D [62]

stacking interactions between these aromatic residues and a sugar molecule are known to contribute largely to the interaction of the protein with the ligand [10]. Glucose molecule also forms 13 hydrogen bonds with the polar residues distributed between the two domains of GGBP [12, 10]. Binding of the sugar molecule inside the ligand-binding site induces a substantial reorganization of the spatial structure of the protein [7, 10]. A "collapse" of the domains of GGBP and their rotation around an axis passing through the 155 and 255 residues of protein can be observed [7, 8]. Changes of the spatial structure of GGBP which accompanies glucose binding can be used in the development of sensitive element of biosensor systems for glucose detection [13–27, 9, 28–34].

Relevant information about the processes of folding, stability and influence on these processes of GGBP ligands, glucose and calcium, was obtained by intrinsic UV fluorescence of proteins [35–44]. As it was shown in these studies, a slight blue shift of the fluorescence spectrum and limited increase in the tryptophan fluorescence intensity of GGBP are observed at the transition of GGBP from the open form (in the absence of ligand) to the closed form (when the sugar molecule is bound) [36]. The change in intrinsic UV-fluorescence of GGBP, which accompanies sugar binding, have been explained by the change of the characteristics of the microenvironment of Trp 183 which is located in the active site of the protein [36].

Fluorescent dyes which were used in the construction of sensitive elements for glucose biosensors were also linked to GGBP in the vicinity of the active center and consequently in the vicinity of Trp 183 [13, 20, 26, 21, 34, 25]. However, while examining binding constant with glucose of one of such potential sensing element we decided to diminish the value of binding constant by changing Trp 183 to Ala. Surprisingly, we found that the response of intrinsic fluorescence of such mutant form to glucose binding is close to the wild type protein. Consequently, we decided to elucidate the reasons of GGPB UV-fluorescence changes on glucose binding. To identify the tryptophan residues of GGBP which are responsible for the increase of the intensity and the blue shift of the fluorescence emission spectrum of the protein upon its binding to D-glucose, we performed the analysis of the microenvironment of tryptophan residues of GGBP in its open state and in complex with glucose.

Materials and Methods

Materials

The wild type of GGBP (GGBPwt) and mutant form GGBP-W183A were obtained, separated and purified as described previously [36]. Briefly, pET-11d plasmids (Stratagene, USA) encoding for GGBPwt and GGBP-W183A mutant were used to transform *E. coli* BL21(DE3) cells. The expression of the proteins was then induced by adding 0.5 mM isopropyl-beta-D-1-thiogalactopyranoside (IPTG; Nacalai Tesque, Japan). Bacterial cells were cultured for 24 h at 37 °C. Recombinant proteins were purified using Ni^{+}-agarose packed in His-GraviTrap columns (GE Healthcare, USA). Protein purification was controlled using denaturing SDS-electrophoresis in 15 % polyacrylamide gel [45].

The experiments were performed in solutions with 0.2 mg/ml protein concentration. For the formation of the

protein–ligand complex, 20 mM of D-glucose was added to the protein solution. D-glucose (Sigma, USA) was used without further purification. The measurements were made in 20 mM PBS buffer (pH 7.4).

Analysis of Protein 3D Structure

An analysis of the microenvironment of tryptophan residues of GGBP was done on the basis of PDB data of GGBP in its open form (2FWO.ent file [7]) and in complex with D-glucose (2FVY.ent file [7]).

The microenvironment of the tryptophan residue was determined as a set of atoms located some distance less than r_0 from the geometrical center of the indole or phenol ring; r_0 was taken to be 7 Å [46, 47]. The nearest atom in the microenvironment to each atom of the indole ring was specified, and the distance between them was determined. The packing density of the atoms in a microenvironment was determined as the part of the microenvironment volume (V_0) occupied by the atoms ($d=\sum V_i/V_0$). The volume occupied by each atom (V_i) was determined according to its van der Waals radius, and only the part inside the microenvironment was taken into account. The real values of atom volume are slightly smaller, as atoms are incorporated in chemical bonds. Nonetheless, it is found to be not significant for the estimation of microenvironment packing density of tryptophan residues.

The efficiency of nonradiative energy transfer between any two tryptophan residues was evaluated as $E = 1/(1+(2/3)/k^2(R/R_0^6))$ [48], where R_0 is the average distance between a randomly orientated donor and acceptor at which $E=0.5$; R is the distance between the geometrical centers of the indolic rings of a donor and an acceptor; and k^2 is the factor of mutual orientation of the donor and the acceptor. The value of k^2 is determined as $k^2=(\cos\theta-3\cos\theta_A\cos\theta_D)^2$. Here, θ is the angle between the directions of the emission oscillator of a donor and the absorption oscillator of an acceptor, θ_D is the angle between the emission oscillator and the vector connecting the geometrical center of the donor, and θ_A is the angle between the absorption oscillator and the vector connecting the geometrical center of the acceptor [49]. The value of R_0 for Trp-Trp pair was taken from the literature [50, 51]. All other parameters were determined according to atoms coordinates [46, 47, 52–54]. Oscillators were considered to be rigid in all calculations.

Fluorescence Measurements

The fluorescence experiments were carried out using a Cary Eclipse spectrofluorimeter (Agilent, Australia). The excitation wavelength for the UV fluorescence spectra was 297 nm. Fluorescence lifetime was measured using a "home built" time resolved spectrofluorimeter [55]. The measurements were made at 23 °C with micro-cells (5×5 mm; Hellma, Germany and 10×10 mm; Starna, Great Britain).

Fluorescence intensity was corrected on the primary inner filter effect according to approach which we recently proposed [56]. It is well known that fluorescence intensity is not proportional to the fluorophore concentration. The nonlinearity of the dependence of the fluorescence intensity on the concentration of a fluorescent substance is caused by the so-called primary inner filter effect. The reasons for this effect are the attenuation of the exciting light flux on its path through an absorbing solution (Beer–Lambert law) and the difference between the area that is illuminated by the exciting light and the working area from which the fluorescence light is gathered.

So, the fluorescence intensity should be always corrected on primary inner filter effect:

$$F_0(\lambda_{ex},\lambda_{em}) = F(\lambda_{ex},\lambda_{em})/W,$$

here, $F(\lambda_{ex},\lambda_{em})$ is the recorded total fluorescence intensity, W is a correction factor, which can be calculated as $W = \frac{1-10^{-A}}{A}$, and A is the absorbance.

In all spectrofluorimeters with vertical slits the area illuminated by the exciting light does not coincide with the working area from which the fluorescence light is gathered. As a result, the detected fluorescence intensity is not proportional to the portion of light absorbed by the solution, and the correction factor cannot be calculated according to the above equation, but must be determined experimentally [56]. At the same time due to horizontal slits in Cary Eclipse spectrofluorimeter the area illuminated by the exciting light and the working area from which the fluorescence light is gathered coincide. That is why this spectrofluorimeter provides the proportionality of the detected fluorescence intensity to the part of the light absorbed by the fluorescent solution and consequently correction factor W can be calculated on the basis of solution absorbance according to the above equation.

It is usually accepted that in the range of fluorophore small concentration fluorescence intensity is proportional to the concentration of fluorescence substance and primary inner filter is negligibly small. Recently we showed that it is not so [56]. Indeed, fluorescence is proportional to absorbance (A) only in one point, when $A=0$. Even at $A=0.1$, the deviation from linearity is 12 %, and at $A=0.3$, it is 38 %! This data clearly indicate the necessity of accounting of the primary inner filter effect.

Stern-Volmer Quenching and Estimating the Bimolecular Quenching Rates

We used acrylamide-induced fluorescence quenching to evaluate the solvent accessibility of the tryptophan residues of the

protein. The intrinsic protein fluorescence was excited at 297, and the emission was monitored at 340 nm. The data generated were corrected based on the solvent signal. The quenching constant was evaluated using the Stern-Volmer equation $q_0/q=1+K_{SV}[Q]$, where K_{SV} is the Stern-Volmer quenching constant, Q is the quencher concentration, and the subscript 0 indicates the absence of a quencher [57]. Consequently, $F[0]/F = \frac{W[0]}{W}(1 + K_{SV}[Q])$, where $W = \frac{1-10^{-A}}{A}$, and A is absorbance [56]. Previous studies have demonstrated the need to include the ratio $W[0]/W$ if the quencher absorbs at the excitation wavelength [58, 59]. The bimolecular quenching rates k_q were calculated from K_{SV} and the mean-square fluorescence lifetime τ using the equation $k_q=K_{SV}/\tau$ ($M^{-1}s^{-1}$) [57].

Circular Dichroism Measurements

The CD spectra were recorded using a Jasco-810 spectropolarimeter (Jasco, Japan). Near-UV CD spectra were recorded in a 10-mm path length cell from 320 nm to 250 nm with a 0.1 nm step size. For the spectra, we recorded 3 scans on average. The CD spectra for the appropriate buffer solution were recorded and subtracted from the protein spectra.

Results and Discussion

The tryptophan fluorescence spectrum of GGBPwt is rather red shifted (λ_{em}=338 nm, λ_{ex}=297 nm, Fig. 2a, Table 1), which is typical for proteins, which tryptophan residues are solvent exposed. At interaction of GGBPwt with D-glucose tryptophan fluorescence spectrum shows 1–2 nm blue shift, and the intensity of tryptophan fluorescence increases (Fig. 2a, Table 1). We have analyzed the spatial structure of GGBPwt [7] in the open form and in complex with D-glucose (GGBPwt/Glc [7]) for correct interpretation of the spectral characteristics of the protein and its complex with the ligand.

Among the five tryptophan residues of the protein, four residues (Trp 127, Trp 133, Trp 183 and Trp 195) are located in the C-terminal domain, a fifth residue Trp 284 is located in the N-terminal domain (Fig. 1). It is obvious that the intrinsic UV fluorescence of GGBPwt should reflect predominantly conformational rearrangements of the C-terminal domain of GGBPwt. Tryptophan residues Trp 127 and Trp 195 belong to the α-helical regions of GGBPwt (5 α-helix, Lys 113 – Ala 128 and 7 α-helix, Asp 184 – Leu 196, respectively). Trp 133 and Trp 183 are a part of the β-turns (T19, Trp 133 – Leu 135 and T22, Ala 181 – Asp 184, respectively). The β-turn T22, that connects the 7th α-helix (Asp 184 - Leu 196) and the 1th β-layer (Lys 172 - Thr 180) of the C-terminal domain, places the Trp 183 residue inside the active site of the protein. Trp 284 belongs to the loop between the 10th α-helix (Asp 257 - Asp 274) and 6th β-layer of this domain (Lys 289 – Val 291).

To determine the accessibility to a solvent of tryptophan residues of GGBPwt we estimated the packing density of the atoms enclosed in the microenvironment of tryptophan residues of GGBPwt. It was found that the Trp 183, which is directly involved in the binding of the sugar molecule, has the highest density of microenvironment compared to other tryptophan residues of GGBPwt (d=0.81, Table S1), even if the protein is in an open form. At complex formation with glucose the density of microenvironment of Trp 183 is increased up to 0.90 (Table S1). This may testify that this residue has the most blue-shifted fluorescence spectrum among the tryptophan residues of the protein and that it is responsible for an increase in intensity and a small blue shift of the tryptophan fluorescence of GGBP at the transition of the protein from the open to the closed form.

The remaining tryptophan residues of GGBPwt have noticeably lower density of the microenvironment and the lowest density of the environment is revealed for the Trp 133 and Trp 284 (Table S1). At protein interaction with the glucose the microenvironment density of these residues of GGBPwt is not altered significantly (Table S1). As it was previously shown by the intrinsic tryptophan fluorescence and differential scanning calorimetry, the interaction of GGBPwt with D-glucose resulted in the overall compaction of the protein structure [36, 35]. Probably, significant changes in the spatial structure of the protein upon complex formation with the ligand do not affect the protein regions that hold these tryptophan residues.

We analyzed the composition of the microenvironment of tryptophan residues of GGBPwt in open and closed forms. The microenvironment of Trp 183 of GGBPwt in an open form is predominantly polar – the sphere with radius in 7 Å from the center of the indole ring of Trp 183 contains 14 atoms of polar residues (including 5 oxygen atoms of the bound water) and only one atom of nonpolar residue Ala 155 (Table S2). This may result in the formation of a relatively red-shifted fluorescence spectrum of Trp 183. Moreover, upon complex formation with glucose the microenvironment of Trp 183 becomes even more polar – in its composition three new polar groups are added: OH group of Tyr 10, OD1 group of Asp 14 and OE1 group of Glu 149 (Table S3). At that, the nitrogen atom NE2 of the His 152 residue and nitrogen atom NH1 of the Arg 158 residue become closer to the indole ring of Trp 183 (to 0.44 and 0.16 Å, respectively). The microenvironment of Trp 183 of GGBPwt/Glc as that of the free protein includes the only hydrophobic group of Ala (Table S3). These data testify that if the fluorescence spectrum of Trp 183 at complex formation of GGBPwt with the ligand is changed, it is most probably become red-shifted.

The microenvironment of a single N-terminal residue of GGBPwt Trp 284 is a polar and most solvent accessible among the all of the tryptophan residues of the protein. At

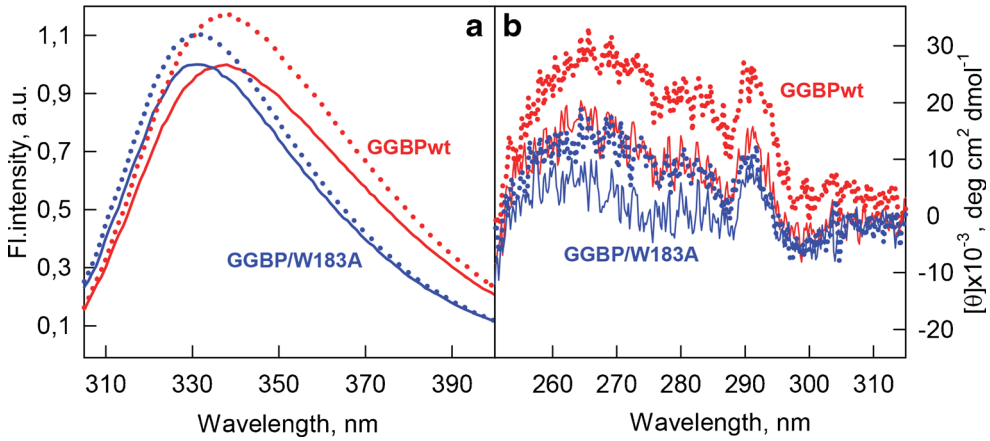

Fig. 2 Tertiary structure of GGBPwt (*red lines*) and its mutant form GGBP-W183A (*blue lines*) in the open state of proteins (*solid lines*) and in the complex with D-glucose (*dotted lines*) tested by intrinsic tryptophan fluorescence (λ_{ex}= 297 nm; panel ***a***) and near-UV CD (panel ***b***)

interaction of GGBPwt with D-glucose the polarity of the microenvironment of Trp 284 is increased by an additional polar group of a Lys 263 residue and five atoms of bound water (Tables S1–S3). This indicates that this residue is characterized by red-shifted fluorescence spectrum and it can not be responsible for the observed change in the spectral characteristics of intrinsic UV fluorescence of GGBPwt at interaction with D-glucose.

The analysis of the microenvironment of Trp 127 and Trp 133 residues of GGBPwt revealed that the efficient nonradiative energy transfer exists between these tryptophan residues (Table S4). This allows us to consider Trp 127 and Trp 133 residues of the protein as a single fluorescent center. The microenvironment of the Trp 127 residue of GGBPwt includes only 3 polar group of the protein and 6 atoms of bound water. An interesting feature of the microenvironment of this residue is the presence of a maximal amount (15, see Table S2) of hydrophobic groups in its composition as compared to the residues Trp 183 and Trp 284 of the protein. At interaction of GGBP with D-glucose the amount of hydrophobic groups in the microenvironment of Trp 127 stays unaltered (Table S3). One molecule of the bound water leaves the microenvironment of the Trp 127 of GGBPwt/Glc, and all polar groups of the microenvironment move from the center of the indole ring to a distance of 0.09–0.13 Å. The microenvironment of the other tryptophan residue Trp 133 of GGBPwt is composed of a large amount of polar groups at the first glance, but only three of them are polar groups of the protein, and it includes a large number of hydrophobic groups (Tables S2–S3). At protein transition to the D-glucose-bound state the microenvironment of Trp 133 undergoes slight changes: it acquires one hydrophobic group CG1 of the Val 206 residue and two molecules of the bound water, which, however, are located at a substantial distance from the indole ring (Table S3).

The analysis suggests that residues Trp 127 and Trp 133 of GGBPwt, as a single fluorescent center, have a hydrophobic microenvironment, compared with the residues Trp 183 and Trp 284 of the protein and should have rather blue-shifted fluorescence spectrum. The microenvironment of the fluorescent center in the GGBPwt/Glc complex becomes more hydrophobic which should result in the formation of even more blue-shifted fluorescence spectra for the Trp 127 and Trp 133 residues.

The microenvironment of the Trp 195 residue of GGBPwt contains five polar groups of the protein, 6 molecules of bound water and a large number of hydrophobic groups (Table S2). In the GGBPwt/Glc complex the microenvironment of the Trp 195 residue becomes more hydrophobic: two hydrophobic groups CB of Leu 146 and CB of Leu 178 are added, while polar residues are moved from the indole ring to a distance of 0.18–0.68 Å (Table S3).

According to the analysis the increase of fluorescence intensity and a blue shift of the tryptophan fluorescence of

Table 1 The characteristics of intrinsic UV-fluorescence of GGBPwt and GGBP-W183A

Probe	λ_{max}, nm (λ_{ex}=297 nm)	Parameter *A* (λ_{ex}=297 nm)	*r* (λ_{ex}=297 nm, λ_{em}=365 nm)	$<\tau^*>$, ns	k_q, 10^9 M^{-1} c^{-1}
GGBPwt	338	1.00	0.15	7.03±0.09	0.66±0.02
GGBPwt/Glc	336–337	1.00	0.16	6.96±0.15	0.27±0.02
GGBP-W183A	332–333	1.58	0.13	4.12±0.09	1.68±0.12
GGBP-W183A/Glc	330–331	1.68	0.14	4.04±0.03	1.86±0.10

*The values of fluorescence life times are an average of three experiments

GGBPwt at the interaction of the protein with the D-glucose are caused by the change in the characteristics of the microenvironment of the three tryptophan residues of the protein: Trp 127, Trp 133 and Trp 195. The Trp 183 residue of GGBPwt, which at first glance is responsible for the observed changes at the transition of the protein from the open form to the closed form, contrary has a red-shifted fluorescence spectrum as compared with the spectra of the Trp 127, Trp 133 and Trp 195 residues, which is additionally red-shifted at the GGBPwt/Glc complex formation.

For experimental confirmation of the results of the analysis of the microenvironment of GGBPwt tryptophan residues we investigated the spectral characteristics of an open and closed formes of GGBP-W183A mutant protein, which does not contain the Trp 183 residue.

It should be noted that fluorescent characteristics of GGBPwt and GGBP-W183A mutant form can be compared only if an amino acid substitution of the Trp 183 for the alanine residue does not disturb the spatial structure which is inherent to the wild type protein. The tertiary structure of both proteins was characterized by recording the CD spectra in the near-UV region (see Fig. 2b, solid lines). The CD spectrum in the near-UV region of GGBPwt has characteristic bands, which are also observed in the CD spectrum in the near-UV region of the mutant protein GGBP-W183A, although the spectrum of the latter protein is somewhat less pronounced. D-glucose binding has the similar effect on both proteins resulting in an increase of the intensity of the bands in the CD spectra in the near-UV region for GGBPwt and its mutant form GGBP-W183A (Fig. 2b, dotted lines). Less pronounced CD spectrum in the near-UV region of GGBP-W183A, containing all characteristic for GGBPwt bands indicates that although the mutant protein possesses the less compact structure compared to the wild type protein, GGBP-W183A preserves the overall spatial structure typical of the wild type protein. The D-glucose binding promotes overall compaction of the spatial structure of the wild type protein and GGBP-W183A mutant.

More detailed characterization of the properties of tryptophan residues of GGBPwt and GGBP-W183A was carried out by analysis of the accessibility of tryptophan residues of these proteins to quenching of the intrinsic fluorescence by acrylamide. The value of the bimolecular constant of quenching of tryptophan fluorescence of GGBPwt ($0.66\pm0.02 * 10^9$ M^{-1} c^{-1}) is lower than the corresponding value for GGBP-W183A ($1.68\pm0.12 * 10^9$ M^{-1} c^{-1}) which indicates that the tryptophan residues of the mutant protein GGBP-W183A are more solvent accessible compared to the residues of GGBPwt. The formation of the complex with D-glucose leads to the increase of shielding of tryptophan residues of GGBPwt (k_q=$0.27\pm0.02 * 10^9$ M^{-1} c^{-1}) and influences insignificantly on the accessibility to the solvent of tryptophan residues of GGBP-W183A (k_q=$1.86\pm0.10* 10^9$ M^{-1} c^{-1}). These data indirectly confirm that spatial structure of GGBP-W183A is less compact as compared with the wild-type protein, as also shown by the CD in the near-UV region (see Fig. 2b). Conversely, we assume that the increase in the value the bimolecular constant of quenching of tryptophan fluorescence for GGBP-W183A is mainly determined by the absence in its structure of Trp 183, which has the greatest density of the microenvironment, both in the protein open form and in its complex with D-glucose (Table S1).

It is worth noting that GGBP-W183A has the lower value of fluorescence anisotropy (r=0.13) as compared to GGBPwt (r=0.15, Table 1). This indicates that tryptophan residues Trp 127, Trp 133, Trp 195 и Trp 284 are more flexible meaning that they are in less dense microenvironment as compared with Trp 183. These data are in good agreement with the analysis of spatial structure of GGBPwt (Table S1).

These experiments corroborate that the spatial structure of GGBPwt does not undergo noticeable alteration at the introduction of substitution of the amino acid Trp 183 for alanine and revealed differences in the spectral characteristics of GGBPwt and GGBP-W183A (Table 1) are caused by the absence of Trp 183 in the mutant protein.

We compare the fluorescent characteristics of GGBPwt and its mutant form GGBP-W183A. The fluorescence spectrum of GGBP-W183A positioned at 332–333 is 5–6 nm blue-shifted relatively the fluorescence spectrum of GGBPwt (Fig. 2a, Table 1). The D-glucose binding with GGBP-W183A produces a small blue shift of the tryptophan fluorescence spectrum and a moderate increase in the fluorescence intensity of the protein which is less pronounced as compared to the wild type protein (Fig. 2a, Table 1). We suppose that the lower amplitude of the change of the fluorescence intensity of GGBP-W183A comparing to GGBPwt at the transition of the proteins from the open form to the closed form is defined by the less compact spatial structure of the mutant protein GGBP-W183A [35].

The obtained data confirm the finding which has been done on the basis of the analysis of the spatial structure of GGBPwt that the tryptophan residues Trp 127, Trp 133 and Trp 195 have the more blue-shifted fluorescence spectra as compared to the spectrum of Trp 183. Having high polar microenvironment both in the free protein and in the complex of the protein with glucose, Trp 183 does not contribute for the observed changes of the spectral characteristics of GGBPwt at its interaction with the ligand.

Acknowledgments This work was supported in part by the Program MCB RAS (K.K. Turoverov), the Scholarships from the President of RF (Olga V. Stepanenko SP-563.2012.4 and A.V. Fonin SP-2390.2012.4), and the Program of Cooperation between RAS and CNR (S. D'Auria and K.K. Turoverov). The funders had no role in study design, data collection and analysis, decision to publish, or preparation of the manuscript.

References

1. Fukami-Kobayashi K, Tateno Y, Nishikawa K (1999) Domain dislocation: a change of core structure in periplasmic binding proteins in their evolutionary history. J Mol Biol 286(1):279–290. doi:10.1006/jmbi.1998.2454
2. Dwyer MA, Hellinga HW (2004) Periplasmic binding proteins: a versatile superfamily for protein engineering. Curr Opin Struct Biol 14(4):495–504
3. Anraku Y (1968) Transport of sugars and amino acids in bacteria. II. Properties of galactose- and leucine-binding proteins. J Biol Chem 243(11):3123–3127
4. Stepanenko O, Fonin A, Kuznetsova I, Turoverov K (2012) Ligand-binding proteins: structure, stability and practical application. Protein structure. InTech, Rijeka, pp 265–290
5. Hazelbauer GL, Adler J (1971) Role of the galactose binding protein in chemotaxis of *Escherichia coli* toward galactose. Nat New Biol 230(12):101–104
6. Chen X, Schauder S, Potier N, Van Dorsselaer A, Pelczer I, Bassler BL, Hughson FM (2002) Structural identification of a bacterial quorum-sensing signal containing boron. Nature 415(6871):545–549. doi:10.1038/415545a
7. Borrok MJ, Kiessling LL, Forest KT (2007) Conformational changes of glucose/galactose-binding protein illuminated by open, unliganded, and ultra-high-resolution ligand-bound structures. Protein Sci 16(6):1032–1041. doi:10.1110/ps.062707807
8. Shilton BH, Flocco MM, Nilsson M, Mowbray SL (1996) Conformational changes of three periplasmic receptors for bacterial chemotaxis and transport: the maltose-, glucose/galactose- and ribose-binding proteins. J Mol Biol 264(2):350–363. doi:10.1006/jmbi.1996.0645
9. Tolosa L (2010) On the design of low-cost fluorescent protein biosensors. Adv Biochem Eng Biotechnol 116:143–157. doi:10.1007/10_2008_39
10. Vyas NK, Vyas MN, Quiocho FA (1988) Sugar and signal-transducer binding sites of the *Escherichia coli* galactose chemoreceptor protein. Science 242(4883):1290–1295
11. Vyas NK, Vyas MN, Quiocho FA (1991) Comparison of the periplasmic receptors for L-arabinose, D-glucose/D-galactose, and D-ribose. Structural and functional similarity. J Biol Chem 266(8):5226–5237
12. Vyas MN, Vyas NK, Quiocho FA (1994) Crystallographic analysis of the epimeric and anomeric specificity of the periplasmic transport/chemosensory protein receptor for D-glucose and D-galactose. Biochemistry 33(16):4762–4768
13. Amiss TJ, Sherman DB, Nycz CM, Andaluz SA, Pitner JB (2007) Engineering and rapid selection of a low-affinity glucose/galactose-binding protein for a glucose biosensor. Protein Sci 16(11):2350–2359. doi:10.1110/ps.073119507
14. de Lorimier RM, Smith JJ, Dwyer MA, Looger LL, Sali KM, Paavola CD, Rizk SS, Sadigov S, Conrad DW, Loew L, Hellinga HW (2002) Construction of a fluorescent biosensor family. Protein Sci 11(11):2655–2675. doi:10.1110/ps.021860
15. Deuschle K, Okumoto S, Fehr M, Looger LL, Kozhukh L, Frommer WB (2005) Construction and optimization of a family of genetically encoded metabolite sensors by semirational protein engineering. Protein Sci 14(9):2304–2314. doi:10.1110/ps.051508105
16. Fehr M, Lalonde S, Lager I, Wolff MW, Frommer WB (2003) In vivo imaging of the dynamics of glucose uptake in the cytosol of COS-7 cells by fluorescent nanosensors. J Biol Chem 278(21):19127–19133. doi:10.1074/jbc.M301333200
17. Ge X, Rao G, Tolosa L (2008) On the possibility of real-time monitoring of glucose in cell culture by microdialysis using a fluorescent glucose binding protein sensor. Biotechnol Prog 24(3):691–697. doi:10.1021/bp070411k
18. Ge X, Tolosa L, Rao G (2004) Dual-labeled glucose binding protein for ratiometric measurements of glucose. Anal Chem 76(5):1403–1410. doi:10.1021/ac035063p
19. Hsieh HV, Pfeiffer ZA, Amiss TJ, Sherman DB, Pitner JB (2004) Direct detection of glucose by surface plasmon resonance with bacterial glucose/galactose-binding protein. Biosens Bioelectron 19(7):653–660
20. Khan F, Gnudi L, Pickup JC (2008) Fluorescence-based sensing of glucose using engineered glucose/galactose-binding protein: a comparison of fluorescence resonance energy transfer and environmentally sensitive dye labelling strategies. Biochem Biophys Res Commun 365(1):102–106. doi:10.1016/j.bbrc.2007.10.129
21. Khan F, Saxl TE, Pickup JC (2010) Fluorescence intensity- and lifetime-based glucose sensing using an engineered high-Kd mutant of glucose/galactose-binding protein. Anal Biochem 399(1):39–43. doi:10.1016/j.ab.2009.11.035
22. Sakaguchi-Mikami A, Taneoka A, Yamoto R, Ferri S, Sode K (2008) Engineering of ligand specificity of periplasmic binding protein for glucose sensing. Biotechnol Lett 30(8):1453–1460. doi:10.1007/s10529-008-9712-7
23. Sakaguchi-Mikami A, Taniguchi A, Sode K, Yamazaki T (2011) Construction of a novel glucose-sensing molecule based on a substrate-binding protein for intracellular sensing. Biotechnol Bioeng 108(4):725–733. doi:10.1002/bit.23006
24. Saxl T, Khan F, Ferla M, Birch D, Pickup J (2011) A fluorescence lifetime-based fibre-optic glucose sensor using glucose/galactose-binding protein. Analyst 136(5):968–972. doi:10.1039/c0an00430h
25. Saxl T, Khan F, Matthews DR, Zhi ZL, Rolinski O, Ameer-Beg S, Pickup J (2009) Fluorescence lifetime spectroscopy and imaging of nano-engineered glucose sensor microcapsules based on glucose/galactose-binding protein. Biosens Bioelectron 24(11):3229–3234. doi:10.1016/j.bios.2009.04.003
26. Thomas J, Sherman DB, Amiss TJ, Andaluz SA, Pitner JB (2007) Synthesis and biosensor performance of a near-IR thiol-reactive fluorophore based on benzothiazolium squaraine. Bioconjug Chem 18(6):1841–1846. doi:10.1021/bc700146r
27. Thomas KJ, Sherman DB, Amiss TJ, Andaluz SA, Pitner JB (2006) A long-wavelength fluorescent glucose biosensor based on bioconjugates of galactose/glucose binding protein and Nile Red derivatives. Diabetes Technol Ther 8(3):261–268. doi:10.1089/dia.2006.8.261
28. Tolosa L, Gryczynski I, Eichhorn LR, Dattelbaum JD, Castellano FN, Rao G, Lakowicz JR (1999) Glucose sensor for low-cost lifetime-based sensing using a genetically engineered protein. Anal Biochem 267(1):114–120. doi:10.1006/abio.1998.2974
29. Weidemaier K, Lastovich A, Keith S, Pitner JB, Sistare M, Jacobson R, Kurisko D (2011) Multi-day pre-clinical demonstration of glucose/galactose binding protein-based fiber optic sensor. Biosens Bioelectron 26(10):4117–4123. doi:10.1016/j.bios.2011.04.007
30. Ye K, Schultz JS (2003) Genetic engineering of an allosterically based glucose indicator protein for continuous glucose monitoring by fluorescence resonance energy transfer. Anal Chem 75(14):3451–3459
31. Ge X, Lam H, Modi SJ, LaCourse WR, Rao G, Tolosa L (2007) Comparing the performance of the optical glucose assay based on glucose binding protein with high-performance anion-exchange chromatography with pulsed electrochemical detection: efforts to design a low-cost point-of-care glucose sensor. J Diabetes Sci Technol 1(6):864–872
32. Veetil JV, Jin S, Ye K (2010) A glucose sensor protein for continuous glucose monitoring. Biosens Bioelectron 26(4):1650–1655. doi:10.1016/j.bios.2010.08.052
33. Fonin AV, Stepanenko OV, Povarova OI, Volova CA, Philippova EM, Bublikov GS, Kuznetsova IM, Demchenko AP, Turoverov KK (2014) Spectral characteristics of the mutant form GGBP/H152C of D-glucose/D-galactose-binding protein labeled with fluorescent dye

BADAN: influence of external factors. PeerJ 2:e275. doi:10.7717/peerj.275
34. Khan F, Pickup JC (2013) Near-infrared fluorescence glucose sensing based on glucose/galactose-binding protein coupled to 651-blue oxazine. Biochem Biophys Res Commun 438(3):488–492. doi:10.1016/j.bbrc.2013.07.111
35. Stepanenko OV, Fonin AV, Morozova KS, Verkhusha VV, Kuznetsova IM, Turoverov KK, Staiano M, D'Auria S (2011) New insight in protein-ligand interactions. 2. Stability and properties of two mutant forms of the D-galactose/D-glucose-binding protein from *E. coli*. J Phys Chem B 115(29):9022–9032. doi:10.1021/jp204555h
36. Stepanenko OV, Povarova OI, Fonin AV, Kuznetsova IM, Turoverov KK, Staiano M, Varriale A, D'Auria S (2011) New insight into protein-ligand interactions. The case of the D-galactose/D-glucose-binding protein from *Escherichia coli*. J Phys Chem B 115(12):2765–2773. doi:10.1021/jp1095486
37. Piszczek G, D'Auria S, Staiano M, Rossi M, Ginsburg A (2004) Conformational stability and domain coupling in D-glucose/D-galactose-binding protein from *Escherichia coli*. Biochem J 381(Pt 1):97–103. doi:10.1042/BJ20040232
38. D'Auria S, Alfieri F, Staiano M, Pelella F, Rossi M, Scire A, Tanfani F, Bertoli E, Grycznyski Z, Lakowicz JR (2004) Structural and thermal stability characterization of *Escherichia coli* D-galactose/D-glucose-binding protein. Biotechnol Prog 20(1):330–337. doi:10.1021/bp0341848
39. D'Auria S, Ausili A, Marabotti A, Varriale A, Scognamiglio V, Staiano M, Bertoli E, Rossi M, Tanfani F (2006) Binding of glucose to the D-galactose/D-glucose-binding protein from *Escherichia coli* restores the native protein secondary structure and thermostability that are lost upon calcium depletion. J Biochem 139(2):213–221. doi:10.1093/jb/mvj027
40. Scognamiglio V, Scire A, Aurilia V, Staiano M, Crescenzo R, Palmucci C, Bertoli E, Rossi M, Tanfani F, D'Auria S (2007) A strategic fluorescence labeling of D-galactose/D-glucose-binding protein from *Escherichia coli* helps to shed light on the protein structural stability and dynamics. J Proteome Res 6(11):4119–4126. doi:10.1021/pr070439r
41. Herman P, Vecer J, Barvik I Jr, Scognamiglio V, Staiano M, de Champdore M, Varriale A, Rossi M, D'Auria S (2005) The role of calcium in the conformational dynamics and thermal stability of the D-galactose/D-glucose-binding protein from *Escherichia coli*. Proteins 61(1):184–195. doi:10.1002/prot.20582
42. Marabotti A, Herman P, Staiano M, Varriale A, de Champdore M, Rossi M, Gryczynski Z, D'Auria S (2006) Pressure effect on the stability and the conformational dynamics of the D-Galactose/D-Glucose-binding protein from *Escherichia coli*. Proteins 62(1):193–201. doi:10.1002/prot.20753
43. Stepanenko OV, Povarova OI, Stepanenko OV, Fonin AV, Kuznetsova IM, Turoverov KK, Staiano M, D'Auria S (2010) Structure and stability of D-galactose/D-glucose-binding protein. The role of D-glucose binding and Ca ion depletion. Spectrosc Int J 24(3–4):355–359
44. Stepanenko OV, Stepanenko OV, Fonin AV, Verkhusha VV, Kuznetsova IM, Turoverov KK (2012) Protein-ligand interactions of the D-Galactose/D-Glucose-binding protein as a potential sensing probe of glucose biosensors. Spectrosc Int J 27(5–6):373–379
45. Laemmli UK (1970) Cleavage of structural proteins during the assembly of the head of bacteriophage T4. Nature 227(5259):680–685
46. Turoverov KK, Kuznetsova IM, Zaitsev VN (1985) The environment of the tryptophan residue in Pseudomonas aeruginosa azurin and its fluorescence properties. Biophys Chem 23(1–2):79–89
47. Kuznetsova IM, Turoverov KK (1998) What determines the characteristics of the intrinsic UV-fluorescence of proteins? Analysis of the properties of the microenvironment and features of the localization of their tryptophan residues. Tsitologiia 40(8–9):747–762
48. Förster T (1960) Transfer mechanisms of electronic excitation energy. Radiat Res Suppl 2:326–339
49. Dale RE, Eisinger J (1974) Intramolecular distances determined by energy transfer. Dependence on orientational freedom of donor and acceptor. Biopolymers 13(8):1573–1605. doi:10.1002/bip.1974.360130807
50. Eisinger J, Feuer B, Lamola AA (1969) Intramolecular singlet excitation transfer. Applications to polypeptides. Biochemistry 8(10):3908–3915
51. Steinberg IZ (1971) Long-range nonradiative transfer of electronic excitation energy in proteins and polypeptides. Annu Rev Biochem 40:83–114. doi:10.1146/annurev.bi.40.070171.000503
52. Turoverov KK, Kuznetsova IM (2003) Intrinsic fluorescence of actin. J Fluoresc 13(1):41–57
53. Stepanenko OV, Kuznetsova IM, Turoverov KK, Huang C, Wang CC (2004) Conformational change of the dimeric DsbC molecule induced by GdnHCl. A study by intrinsic fluorescence. Biochemistry 43(18):5296–5303
54. Giordano A, Russo C, Raia CA, Kuznetsova IM, Stepanenko OV, Turoverov KK (2004) Highly UV-absorbing complex in selenomethionine-substituted alcohol dehydrogenase from Sulfolobus solfataricus. J Proteome Res 3(3):613–620
55. Turoverov KK, Biktashev AG, Dorofeiuk AV, Kuznetsova IM (1998) A complex of apparatus and programs for the measurement of spectral, polarization and kinetic characteristics of fluorescence in solution. Tsitologiia 40(8–9):806–817
56. Fonin AV, Sulatskaya AI, Kuznetsova IM, Turoverov KK (2014) Fluorescence of dyes in solutions with high absorbance. Inner filter effect correction. PLoS One 9(7):e103878. doi:10.1371/journal.pone.0103878
57. Eftink MR (1994) The use of fluorescence methods to monitor unfolding transitions in proteins. Biophys J 66(2 Pt 1):482–501
58. Sulatskaya AI, Povarova OI, Kuznetsova IM, Uversky VN, Turoverov KK (2012) Binding stoichiometry and affinity of fluorescent dyes to proteins in different structural states. Methods Mol Biol 895:441–460
59. Stepanenko OV, Stepanenko OV, Kuznetsova IM, Shcherbakova DM, Verkhusha VV, Turoverov KK (2012) Distinct effects of guanidine thiocyanate on the structure of superfolder GFP. PLoS One 7(11):e48809
60. Dutta S, Burkhardt K, Young J, Swaminathan GJ, Matsuura T, Henrick K, Nakamura H, Berman HM (2009) Data deposition and annotation at the worldwide protein data bank. Mol Biotechnol 42(1):1–13
61. Hsin J, Arkhipov A, Yin Y, Stone JE, Schulten K (2008) Using VMD: an introductory tutorial. Curr Protoc Bioinforma Chapter 5: Unit 5 7
62. Merritt EA, Bacon DJ (1977) Raster3D: photorealistic molecular graphics. Methods Enzymol 277:505–524